Problems on fabrication of computer-generated holograms for testing aspheric surfaces

Jun Ma (马 骏)[1], Zhishan Gao (高志山)[1], Rihong Zhu (朱日宏)[1*], Yong He (何 勇)[1], Lei Chen (陈 磊)[1], Jianxin Li (李建欣)[1], E. Y. B. Pun (潘裕斌)[2], W. H. Wong[2], Lihui Huang (黄立辉)[2], Changqing Xie (谢常青)[3], Xiaoli Zhu (朱效立)[3], and Jie Ma (马 杰)[3]

[1]*Department of Optical Engineering, Nanjing University of Science and Technology, Nanjing 210094*

[2]*Department of Electronic Engineering, City University of Hong Kong, Kowloon Tang, Hong Kong*

[3]*Key Laboratory of Nano-Fabrication and Novel Devices Integrated Technology, Institute of Microelectronics, Chinese Academy of Sciences, Beijing 100029*

[*]*E-mail: zhurihong@mail.njust.edu.cn*

Received January 22, 2008

Interferometric optical testing using computer-generated hologram (CGH) can give highly accurate measurement of aspheric surfaces has been proved. After the system is designed, a phase function is obtained according to the CGH's surface plane. For the requirement of accuracy, an optimization algorithm that transfers the phase function into a certain mask pattern file is presented in this letter, based on the relationship between the pattern error of CGH and the output wavefront accuracy. Then the writing machine is able to fabricate such a mask with this kind of file. With that mask, an improved procedure on fabrication of phase type CGH is also presented. Interferometric test results of an aspheric surface show that the whole test system obtains the demanded accuracy.

OCIS codes: 220.1250, 050.1970, 090.1760, 220.3620.

doi: 10.3788/COL20090701.0070.

Among several kinds of the aspheric surface test, interferometry is a well-known and high precision method in which phase type computer-generated hologram (CGH) is used to instead the conventional compensator[1]. In order to ensure low thermal expansion and high index homogeneity during the optical system design, fused silica is chose to be the CGH substrate and set the thickness to 5 mm. Although the structure of CGH looks like that of the normal phase type Fresnel zone-plate, the fabrication processes of them are different. The fabrication of normal phase type Fresnel zone-plate includes two procedures, fabrication of mask and etching procedure. In the past, much research work based on the semiconductor industrial technology was focused on the production of large scale integrated circuit on Si substrate or the fabrication of Fresnel zone plate[2] on the normal substrate with small aperture or low spatial frequency. The fabrication of some kinds of diffractive phase type elements with large aperture is based on the holographic exposure technology. It is found that the precision of pattern position generated by the traditional procedure is far from the requirement of accuracy. In addition, the traditional etching procedure[3] cannot be followed for the incompatibility between our substrate and writing machine's chamber. So in this letter, the method of improving the precision of mask pattern is studied. And the research also includes the method of phase type CGH's fabrication with fused silica substrate.

The aperture of CGH is designed as small as possible to achieve the measurement of aspheric surfaces with large aperture[4]. And the result of optical design is only a phase function on CGH's plane surface which adds certain phase to the input wavefront in order to let output wavefront normally incidence onto the aspheric surface under test. The curve in Fig. 1 shows the relationship between the phase in period and the radial position of CGH. Here we make a change to the traditional fabrication procedure[6,7] by adding a transitional operation which transfers the result of optical design to a fabricable format with higher precision. Some problems will be solved in transitional operation procedure with a simple optimization fitting algorithm. These problems include: 1) the relationship between the pattern error and wavefront phase error; 2) how to improve the accuracy of the mask pattern. After that, the laser direct writing machine is used together with this transitional result to generate a mask. In the second procedure, normal fabrication of such phase type binary profile becomes very simple by directly etching the substrate down to a certain depth. But this procedure is only fit for the mask substrate itself whose thickness is 2.28 mm. For 5-mm-thick substrate, it can not be followed any more. And another problem is also included; 3) how to work out the

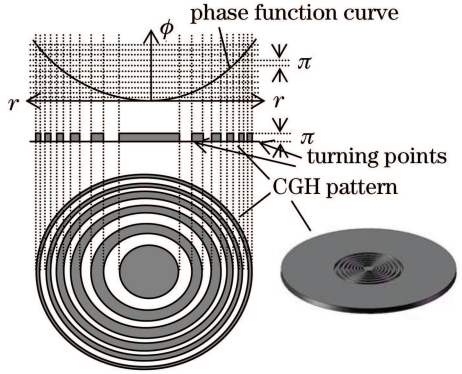

Fig. 1. Phase function curve of CGH and its profile.

phase type binary profile through a modified fabrication procedure.

The prescription of a binary profile includes turning point position and step depth. The turning points' coordinates have to be worked out for the binary planar profile based on

$$\phi(\rho) = \sum_{i=1}^{n} a_i \rho^{2i}, \tag{1}$$

where n is the number of polynomial coefficients in series, ρ is the normalized radius of the maximum distance from the optical axis, and a_i is the coefficient on the $2i$th power of ρ. Then depth problem will be discussed later. Equation (1) shows the phase function as the result of optical design by ZEMAX. This phase function shows that the element will add such a continuous phase to the input wave on the first diffraction order. And values of a_i are obtained as the result. Figure 1 shows the relationship between the phase function and binary step turning point. Every turning point is the intersection point of phase function curve and the corresponding constant phase. The planar profile is a concentric circles structure which is similar to the Fresnel zone-plate. The difference is that it will not give a foci but a caustic which will normally incidence onto the aspheric surface under the test. We use the series of a_i to calculate the radius of each single circle. As shown in Fig. 1, the black is opaque and the parts between the black are transparent on mask. So writing machine is used to write the black part. But arc is not included in the vocabulary of writing machine, and it can only use the combination of rectangles to fit the arc. This fitting process introduces deviation, which leads to wavefront error. Now we are going to introduce the relationship between them, starting from the analysis of wavefront error.

Figure 2 is a simple model for the numerical analysis of wavefront error, where the dotted line is the ideal phase curve and the solid line is the real phase curve. The deviation between them is caused by the pattern error. $\zeta(x, y)$ represents the deviation of pattern's turning points. $\upsilon(x, y)$ is the local spatial frequency of the CGH's binary profile. W_{pe} is the wavefront error at position $r(x, y)$. So $\zeta(x, y) \times \upsilon(x, y)$ gives the total period number of deviation at the position $r(x, y)$. The calculation algorithm of the local wavefront error due to the pattern deviation[6] can be written as

$$W_{\mathrm{pe}} = -m_{\mathrm{R}} \lambda \zeta(x, y) \upsilon(x, y), \tag{2}$$

where m_{R} represents the diffraction order. For example, if $m_{\mathrm{R}} = 1$, the pattern deviation is 10^{-4} mm and the local spatial frequency is 50 lp/mm, thus the wavefront error

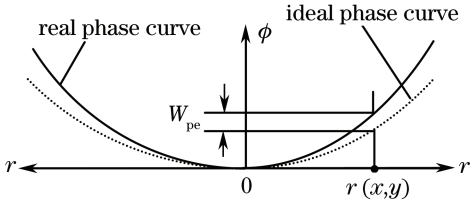

Fig. 2. Deviation between real phase curve and ideal phase curve.

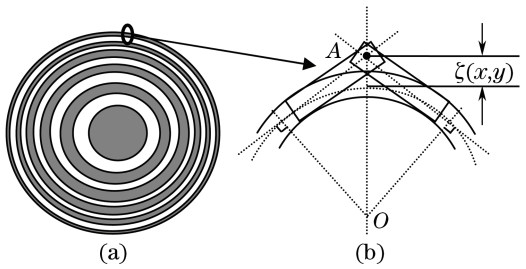

Fig. 3. (a) Diagram of arc fitting and (b) enlarged region shows the deviation.

is $-\lambda/200$.

As described before, if the laser direct writing machine is used to fabricate the mask, it is necessary to divide every ring into the combination of rectangles[7−9]. Fitting process is briefly shown in Fig. 3(a) and the magnified view of a small part of the whole mask is shown in Fig. 3(b). Local ring pattern is an ideal one according to the result of optical design. Two rectangles generated by the writing machine are used to replace the arc. According to the geometry principle, we obtained

$$\zeta(x, y) = \left(\frac{1}{\cos\left(\frac{2\pi}{N}\right)} - 1 \right) r(x, y), \tag{3}$$

where N is used as the fitting number for real pattern, $\zeta(x, y)$ is the fitting deviation which can be considered as the pattern error, $r(x, y)$ is the radius of the intersection point of two rectangles.

This equation is only applicable for the intersection point such as point A in Fig. 3, which has the largest deviation from its original position. Other points do not generate as large wavefront error as the intersection point does. So we only focus on the former one. As described before, pattern error will directly generate local wavefront error.

From Eqs. (2) and (3), it is found that $\zeta(x, y)$ and $\upsilon(x, y)$ are two key factors that affect the result. The larger they are, the worse they generate the wavefront error at the intersection point. To improve the wavefront accuracy, it would be better to decrease both of them. $\upsilon(x, y)$ has no relationship with geometry transitional process. It only depends on the phase change between the input and output wavefront of CGH. From Eq. (1), the phase change is already decided in optical design. So if this factor needs to be decreased, it may be taken into account during system's initial optical design. Actually, the spatial frequency is always connected with the component's effective aperture which also needs to be decreased. But in fact, when one of them is decreased, the other will become larger accordingly. So in order to obtain a better result of fitting deviation during optical design, more attention has to be paid to decrease the CGH's spatial frequency at the cost of generating a little larger aperture. Equation (3) shows that if $\zeta(x, y)$ needs to be decreased, N should be increased to optimize the output wavefront accuracy. But, at the same time, the total division number of the whole mask also has to be suppressed to make sure that it will not be a burden for laser writing pre-processing. So N should be a variable along the radial direction which is the key point of this work. Target wavefront accuracy which is about $\lambda/20$

is set for Eq. (2) based on system's requirement. The spatial frequency $\upsilon(x, y)$ at point $r(x, y)$ is figured out from Eq. (1). The deviation tolerance is obtained for Eq. (3). Finally, a proper division number is worked out for a certain radius. Along the radial direction through this method, a sequence of proper division number which can be used for the arc fitting is obtained. With this division number and corresponding radius, coordinates of every vertex of polygon throughout the whole element can be worked out. These coordinates are the foundation of the mask fabrication.

Figure 4 shows the wavefront error curve along the radial direction. When division numbers are set to be 90, 180, and 360, respectively, the wavefront error gets larger and larger when the radial position moves from central to edge. The dotted straight line which crosses the curve represents the required wavefront accuracy. According to the above analysis, the division number is increased to make sure that the curve can be bent down under the straight line. Figure 5 shows the results after optimization that division number is variable from central to edge. In Fig. 5, the solid curve shows the division number changes from 200 to 800 with the radial position, and the dotted curve shows the wavefront error varies with the radial position. All the points on wavefront error curve are under the required accuracy line. The curve seems to fluctuate around a certain line because the division number is an integer not a float. Figure 5 only shows the wavefront error at every intersection point which contains the most serious pattern error. Obviously, the rest points do not have such serious error, but they are also improved after optimization.

During the optical design and the above transitional procedure, we get the relationship among several parameters of CGH, including its effective aperture, spatial frequency, and total number of polygons. Using laser direct writing machine, a 4 inches mask with designed pattern is fabricated. The substrate of this mask is soda lime, a kind of normal glass in clean room. Actually, normal binary stair-case profile can be achieved by etching the mask down to a certain depth directly. But now, when fused silica is chosen instead, it has to be fabricated through a new method. And several parameters of binary profile are decided including etching depth[10], duty circle, and transparency of high and low level[11]. Phase level which decides the number of grating level is set to be one for binary grating. The relationship between phase level and phase difference can be written as

$$\phi = \frac{2\pi}{2^{N_{\mathrm{div}}}}, \tag{4}$$

where ϕ is the phase difference between two levels, N_{div} is the division number. The determination of binary profile's depth according to optical path difference that comes from phase difference between two levels can be written as

$$\frac{h(n-1)}{\lambda} = \frac{\phi}{2\pi}, \tag{5}$$

where λ is the working wavelength, n is the refractive index of the substrate. For our system, He-Ne laser whose wavelength is 632.8 nm is used and the refractive index of fused silica at this wavelength is 1.4572. So the depth h is 692 nm. New fabrication procedure contains three steps as shown in Fig. 6. Firstly, magnetic sputtering system is used to coat a layer of metal on the substrate. Secondly, mask's pattern is copied to substrate's metal layer. So the rest metal can cover unwanted etched substrate. Finally, reactive ion etch (RIE) machine is used to etch the uncovered substrate down to the designed depth. Figure 7 shows the etching result measured with a step profile facility and Fig. 8 shows the photo of the fabricated phase type CGH element. After removing the rest metal, the phase type CGH is obtained.

Together with phase shifted Fizeau interferometer CXM-100 and transmission sphere $F/3.3$, it is able to test the aspheric surface with the prescription in Table 1. Figure 9 shows the interferogram and test result. And Fig. 10 shows the result obtained with Taylor Hobson's profilometer. Two results are basically in agreement with each other.

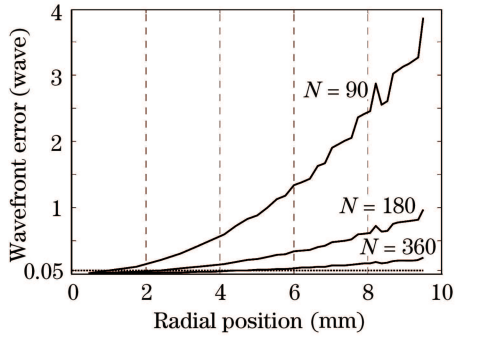

Fig. 4. Wavefront error versus fitting number N.

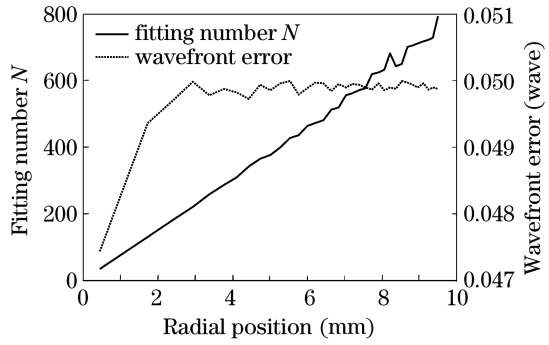

Fig. 5. Fitting number N versus radial position and the wavefront error after optimization.

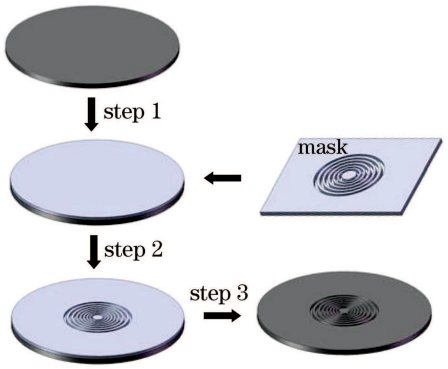

Fig. 6. Fabrication procedure.

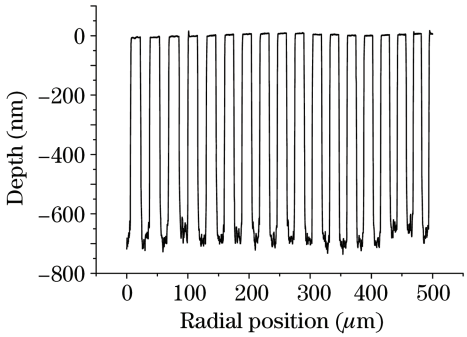

Fig. 7. Curve of the etching depth.

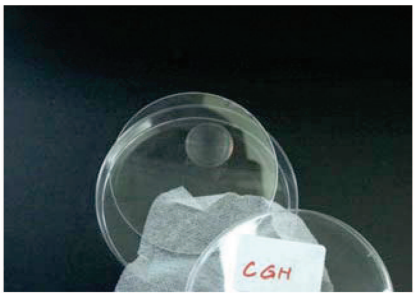

Fig. 8. Picture of the phase type CGH.

Table 1. Prescription of Aspheric Surface

R_0 (mm)	K	A_4	A_6
−158.47	0	2.32×10^{-8}	2.54×10^{-12}

Fig. 9. Interferogram obtained with CGH and CXM-100.

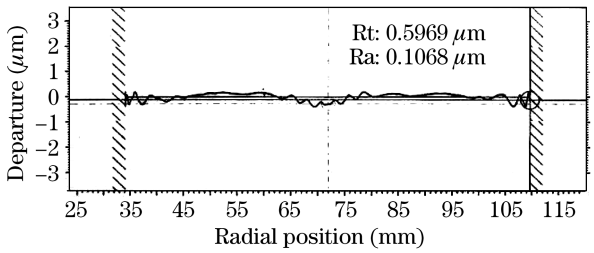

Fig. 10. Scanning profile of Taylor Hobson's profilometer.

In conclusion, a transitional method from optical design to CGH's mask fabrication is obtained. A new fabrication procedure of the phase type CGH with 5-mm thick fused silica substrate is also presented. The optimization fitting algorithm ensures the output wavefront accuracy from the CGH. And the fabrication procedure makes it possible to use fused silica as the substrate with the thickness of 5 mm.

The authors thank S. M. Arnold of Diffraction International for his invaluable discussion.

References

1. H. J. Tiziani, S. Reichelt, C. Pruss, M. Rocktashel, and U. Hofbauer, Proc. SPIE **4440,** 109 (2001).
2. W. H. Wong and E. Y. B. Pun, J. Vac. Sci. Technol. B **19,** 732 (2001).
3. I. Steingoerrer, A. Grosse, and H. Fouckhardt, Proc. SPIE **4984,** 234 (2003).
4. Z. Gao, M. Kong, R. Zhu, and L. Chen. Chin. Opt. Lett. **5,** 241 (2007).
5. E. Bernhard Kley, W. Rockstroh, H. Schmidt, A. Drauschke, F. Wyrowski, and L. Witting, Proc. SPIE **4440,** 135 (2001).
6. A. Fercher, Opt. Acta **23,** 347 (1976).
7. I. Kallioniemi, J. Saarinen, K. Blomstedt, and J. Turunen, Appl. Opt. **36,** 7217 (1997).
8. Z. Chen, Y. Vladimirsky, M. Brown, Q. Leonard, O. Vladimirsky, F. Moore, B. Lai, W. Yun, and E. Gluskin, J. Vac. Sci. Technol. B **15,** 2522 (1997).
9. S. M. Arnold, Proc. SPIE **2536,** 117 (1995).
10. H. P. Herzig, (ed.) *Micro-Optics: Elements, Systems and Applications* (Taylor & Francis Ltd., London, 1997, Reprinted 1998) p.30.
11. Y. Chang and J. H. Burge, Proc. SPIE **3782,** 358 (1999).